ELSEVIER

Journal of Photochemistry and Photobiology A: Chemistry 104 (1997) 133–139

Journal of PHOTOCHEMISTRY AND PHOTOBIOLOGY A:CHEMISTRY

Photocurrent kinetics (in the microsecond time range) of chlorophyll *a*, chlorophyll *b* and stilbazolium merocyanine solutions in a nematic liquid crystal located in an electrochemical cell

A. Ptak [a,b], A. Der [a], R. Toth-Boconadi [a], N.S. Naser [b], D. Frąckowiak [b,*]

[a] *Institute of Biophysics, Biological Research Centre, Szeged 8701, Hungary*

[b] *Poznań Technical University, Molecular Physics Laboratory, Institute of Physics, ul. Piotrowo 3, 60-696 Poznań, Poland*

Received 15 July 1996; accepted 23 September 1996

Abstract

The photosynthetic pigments chlorophyll *a* and chlorophyll *b* solutions in a nematic liquid crystal were located between semiconducting and metallic transparent electrodes and illuminated by lamp or laser light. Cells with two semiconducting electrodes were also investigated. Such systems represent models of biological membranes simulating their fluid and oriented structure. The kinetics of photocurrent generation in the time range from microseconds to minutes were measured. The action spectrum of the photocurrent effect was established. The kinetics of the photocurrent generated by laser flash photolysis in the chlorophyll solutions are complex and to some extent similar to the kinetics reported for thylakoids. For comparison, the photocurrent kinetics of stilbazolium merocyanine, a highly protonated dye, were also measured. In this case, on flash illumination, only one photocurrent peak was observed. This peak is due to electron tunnelling to the semiconducting electrode. In the case of chlorophylls, several effects, such as charge displacement and migration of the ions, are superimposed giving a complex photocurrent generation. The results suggest that, in the case of chloroplasts, the kinetics of photopotential generation may be partially dependent on the membrane structure and fluidity. © 1997 Elsevier Science S.A.

Keywords: Chlorophyll; Electrochemical cell; Liquid crystal; Merocyanine; Photocurrent

1. Introduction

In recent years, several investigations of the charge transfer and migration in photosynthetic organisms have been undertaken. The photoelectrochemical effects were generated by very short flashes of light [1–7]. The illumination of pigmented membranes of photosynthetic organisms leads to the generation of an electrical potential difference between the two surfaces of the membranes. These photopotentials, observed for dense suspensions of thylakoids, are explained as being due predominantly to the lack of compensation between the photoelectrons generated on the sides of the discs exposed to stronger illumination and those generated on the sides of the discs located further away from the light source [1,2,4–6]. This is called the light gradient effect [4]. Certain secondary effects, such as the change in the sign of the signal as a function of the light wavelength, were explained by light interference [5]. The dependence of the sign of the photopotential on the side of sample illumination, observed for magnetically oriented chloroplasts [7], may suggest that the membrane structure has some influence on electrogenic reactions.

Living organisms are complex systems containing several mutually interacting species and an incompletely known structure. Therefore the mechanisms responsible for photoelectrochemical effects can be more easily established by the investigation of model systems. In this paper, electrochemical effects are investigated on liquid crystal (LC) solutions, i.e. on simpler systems simulating to some extent the properties of biological membranes. LCs are fluid and can be oriented easily [8–11]. The dielectric properties of chlorophyll (Chl) solutions in LCs are known [12]. The orientations of Chl transition moments with respect to LC molecules have been established previously [8]. Chl *a* and *b*, as obtained by resonance Raman spectroscopy, exist in LCs mostly as solvated monomers with pentacoordinated Mg atoms [13]. They are photochemically stable in such solvents [8,9,13]. The application of an electric or magnetic field changes the orientation of the LC and pigment molecules in the same manner [14]

Abbreviations: Chl, chlorophyll; EBBA, *p*-ethoxybenzylidieno-*p*-butylaniline; LC, liquid crystal; MBBA, *p*-methoxybenzylidieno-*p*-butylaniline

* Corresponding author. Tel.: +48 61 782344; fax: +48 61 782324.

PII S1010-6030(96)04508-X

because of the "guest–host" effect. The photoelectrical properties of Chls and merocyanine in an LC solvent in the seconds time range have been investigated [10,11,15,16]. The electrochromic effects of both types of pigment were observed at a much higher electrical field than that generated at a semiconducting electrode [12,17]. Chl in a non-illuminated electrochemical cell is non-ionized [8,9]. Pigment molecules which are located in an electric field gradient due to a semiconducting electrode–sample junction can be ionized by illumination with visible light [18].

Photoelectrical effects are observed not only for pigmented biological membranes [3,4,6,19,20], but also for artificial systems constructed in order to convert light energy into electrical energy [21]. Several attempts have been made to apply pigments and pigment–protein complexes, separated from organisms, in arrangements proposed for energy conversion [21]. The mechanisms responsible for charge generation in both biological and artificial systems are similar.

Previously [10,11], for the same set of dyes as used in this study, located in nematic LCs, but illuminated with white light, the kinetics of photopotential and photocurrent generation were measured in the seconds time range. In this paper, faster kinetics (microseconds after the laser pulse) are reported and compared with previous literature data concerning LC electrochemical cells [10,11,22–24] and with the photopotentials of organisms or their fragments [3,4,6]. In order to establish the effects occurring for molecules charged in the dark, stilbazolium merocyanine, which is highly protonated in LCs [16], was investigated.

2. Materials and methods

Chl *a* and *b* were purified chromatographically according to the method described in Ref. [25]. Stilbazolium merocyanine (1-(6'-hydroxyl)-4-[(3,5-di-tert-butyl-4-oxycyclohexa-2,5-dienylidene)ethylidene]) was obtained from Professor Ilona Gruda. The pigments were dissolved in a nematic LC mixture of *p*-methoxybenzylidieno-*p*-butylaniline (MBBA) and *p*-ethoxybenzylidieno-*p*-butylaniline (EBBA) (3:2). Both LCs (from E. Merck, Darmstadt) were used without purification. Solutions of two concentrations (10^{-3} and 10^{-4} M) were prepared. The solutions of the pigments were located in electrochemical cells. Two types of cell were used: one with both windows covered by semiconducting In_2O_3 layers, and the other with one semiconducting In_2O_3 electrode and one electrode with a transparent gold layer deposited in vacuo. Three cell thicknesses were used: 10, 20 and 60 μm.

Two types of experiment were carried out using arrangements similar to those described in Refs. [6,26–28]. In the first type of experiment (Fig. 1(A)), the sample was excited with a projector lamp with a shutter through interference filters. The kinetics of generation and decay of the photocurrent after switching the light on and off at various wavelengths were recorded. The saturation of the signal was reached in

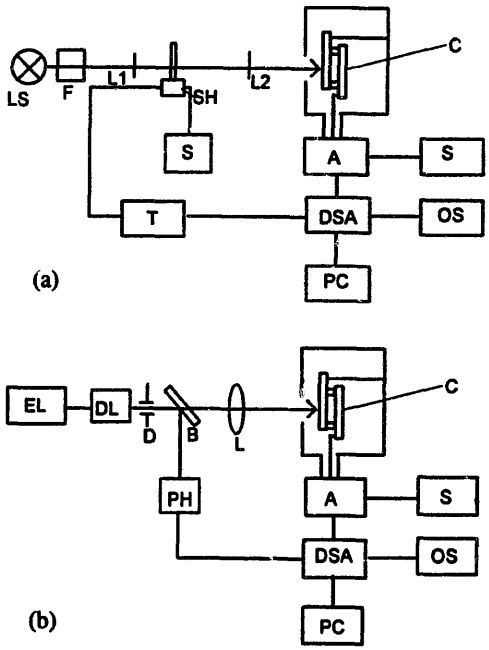

Fig. 1. Arrangements used in the photocurrent measurements: (A) LS, lamp; F, filter; SH, shutter; S, power supply; C, sample; A, amplifier; T, timer; DSA, digital storage adaptor (DSA524, Thurlby); PC, personal computer; Os, oscilloscope; L, lens. (B) EL, excimer laser; DL, dye laser; PH, photodiode; C, sample; B, beam splitter (other notations as in (A)).

similar times; therefore the current intensities at the same time at various wavelengths can be used to calculate the action spectrum. In the calculation of the action spectrum, the spectral distribution of the emitted light and the transmission of the filters were taken into account. The electric signals were traced by a digital storage adaptor and an oscilloscope with a home-built pre-amplifier of 10 MHz and 1 MΩ input impedance. Data were stored and analysed by a personal computer.

In the second type of experiment (Fig. 1(B)), the samples were excited with a dye laser pumped by an excimer laser (EMG 101 MSC, Lambda Physik, Germany). The laser pulse duration was about 20 ns. Different wavelengths were selected using the following dyes: stilbane 3 (410–454 nm; maximum, 424 nm), rhodamine 6G (569–606 nm; maximum, 580 nm) and DCMLC 65001 (631–690 nm; maximum, 658 nm) (Lambda Physik, Germany). The light energy was measured with a home-built Joule meter based on an ED-100A sensor (Gentec Inc., Canada). The laser flash (energy different for various dyes: 270×10^{-6} J for stilbane 678×10^{-6} J for DCMLC 65001 and about 1160×10^{-6} J for rhodamine 6G; pulse duration, 20 ns) was defocused in such a way that the surface of the sample, with a diameter of 10 mm, was uniformly illuminated.

3. Results and discussion

3.1. Experiments with a projection lamp

Fig. 2 shows the action spectra of photocurrent generation for the pigment solutions in LC and for LC alone. Spectra

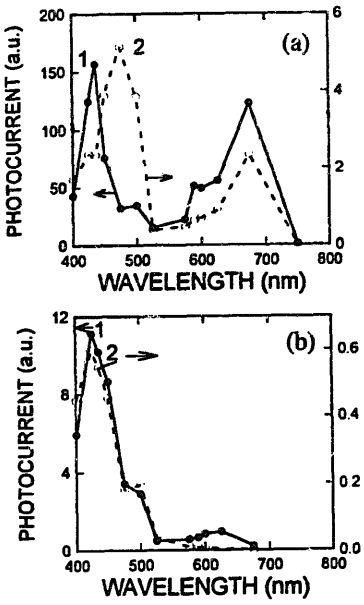

Fig. 2. Action spectra of photocurrent generation: (A) curve 1 (left scale), Chl *a* in LC between Au and In_2O_3 electrodes; curve 2 (right scale), Chl *b* in LC between two In_2O_3 electrodes; (B) curve 1 (left scale), merocyanine in LC; curve 2 (right scale), LC alone (both between Au and In_2O_3 electrodes). All a.u. are the same.

were taken on illumination of the sample with the projector lamp with a shutter and were corrected as described in Section 2. In Fig. 2, only the absolute values of the current amplitude, not the sign of the photocurrent, are shown. The shapes of the action spectra for Chl *a* and Chl *b* (Fig. 2(A)) are similar to the absorption spectra of the same solutions reported previously [9,29]. The maximum of the photocurrent action spectrum of the LC cell is located at about 430 nm. The amplitude of the photocurrent of LC alone (Fig. 2(B), curve 2, right scale) is much lower than that for all pigmented cells. The Chl *b* action spectrum (Fig. 2(A), curve 2, right scale) was taken for a sample located between two semiconducting electrodes (In_2O_3), whereas the Chl *a* solution (Fig. 2(A), curve 1, left scale) was measured in an asymmetric cell with Au and In_2O_3 electrodes. The asymmetric cell for the same sample gives a much higher amplitude than the symmetric cell with two semiconducting electrodes. The short-wavelength part of the merocyanine action spectrum (Fig. 2(B), curve 1, left scale) (maximum at 430 nm) is due to the superposition of the absorption of the protonated form of the dye [16] and the very low LC effect. In the 580–680 nm region, only the absorption of the free base merocyanine form is responsible for the photocurrent. In LC, the ratio of free base to protonated forms of stilbazolium merocyanine is very low (about 0.05) [16]. The photocurrent effect of Chls is stronger than that of protonated merocyanine. The evaluation of the photocurrent and absorption ratios for both merocyanine forms shows that the free base form is more effective in photocurrent generation than the protonated form.

Fig. 3 shows the kinetics of photocurrent generation after switching the lamp on and off for unpigmented LC located between Au and In_2O_3 electrodes. The generation (τ_g) and decay (τ_d) times calculated assuming a monoexponential course were about 0.7 s and 0.9 s respectively. Unpigmented cells exhibit a faster decay of the photopotential than cells pigmented with Chls. The signal amplitude increase after switching the light on (from 4.2 to 4.8 s) is much faster than the decay (from 7 to 11 s) for all pigmented samples (Fig. 4), which is in agreement with results reported previously for similar samples [10,11]. The times of the photopotential

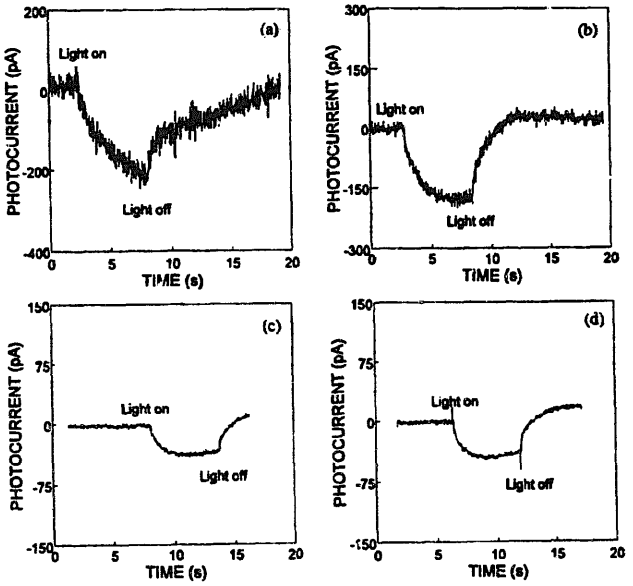

Fig. 3. Kinetics of photocurrent generation and decay in unpigmented LC in the asymmetric cell. Light wavelength: (a) $\lambda = 436$ nm; (b) $\lambda = 450$ nm; (c) $\lambda = 500$ nm; (d) $\lambda = 525$ nm (time of signal generation $\tau_g \approx 0.7$–1.0 s; decay time $\tau_d \approx 1.0$–1.3 s). The value of the dark current was taken as zero.

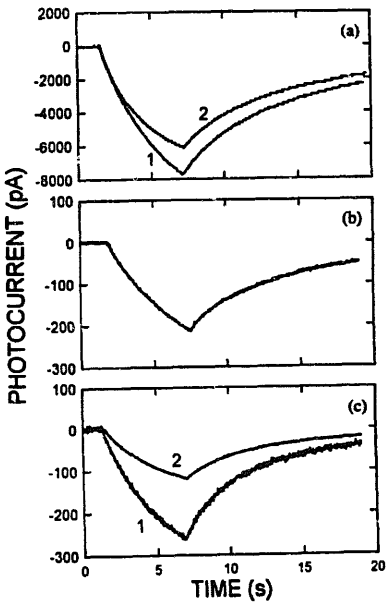

Fig. 4. Kinetics of photocurrent generation and decay: (A) Chl *a* in LC in asymmetric Au/In_2O_3 cell; curve 1, $\lambda = 425$ nm ($\tau_g \approx 4.6$ s, $\tau_d \approx 10.0$ s); curve 2, $\lambda = 675$ nm ($\tau_g \approx 4.8$ s, $\tau_d \approx 11.0$ s); (B) Chl *a* in LC between two semiconducting electrodes; $\lambda = 675$ nm ($\tau_g \approx 4.2$ s, $\tau_d \approx 8.5$ s); (C) Chl *b* in LC symmetric cell; curve 1, $\lambda = 475$ nm ($\tau_g \approx 4.2$ s, $\tau_d \approx 5.5$ s); curve 2, $\lambda = 675$ nm ($\tau_g \approx 4.6$ s, $\tau_d \approx 7.3$ s)

increase and decay for various pigmented samples are given in Figs. 3-5. From Fig. 2(B), it can be seen that the photocurrent of the unpigmented LC cell is measurable only in the short-wavelength region (up to 525 nm) in a cell with two different electrodes. When the metal counter-electrode is grounded, the sign of this effect is always negative, as shown in Fig. 3. This is in agreement with literature data concerning unpigmented LC cells [23].

The amplitudes of the signals generated in a similar arrangement for LC pigmented by Chl *a*, Chl *b* or merocyanine are also negative, but much higher than that observed for LC alone. All the experiments show that electrons are tunnelled from the excited molecules to the semiconducting electrode. The kinetics of the same samples in symmetric cells are shown in Fig. 4(B) for Chl *a* and Fig. 4(C) for Chl *b*.

When the same type of sample is located between two semiconducting electrodes in several cells, different directions and amplitudes of the signals are observed for the various cells. Asymmetric cells give stronger and more reproducible signals. When, for the same cell, measurements were performed by first grounding the dark back electrode and illuminating the front electrode and then grounding the front electrode and illuminating the back electrode, the amplitudes of the effect were similar, but the sign was changed. These effects can be caused by the nonidentical properties of various semiconducting electrodes or by an asymmetric distribution of charge in the cell caused by previous illumination. The charge distribution on illumination slowly decays during several hours of cell dark storage. A similar experiment with a change in role of the electrodes in the case of an asymmetric cell (Au/In_2O_3) always gives negative signals for Chls when the Au electrode is grounded and the semiconducting electrode is illuminated, and a similar effect when the side of illumination of the electrodes is changed. Similar current amplitudes were observed on both sides of illumination. The charges are generated in the vicinity of the semiconducting electrode [18,29], and therefore a similar effect on illumination of both sides of the cell suggests that the light gradient only weakly influences the photocurrent generation in the investigated cells on steady state illumination. The light gradient effect was observed in an arrangement with modulated light [30], where the effects occurring a short time after cell illumination contributed mainly to the measured signal.

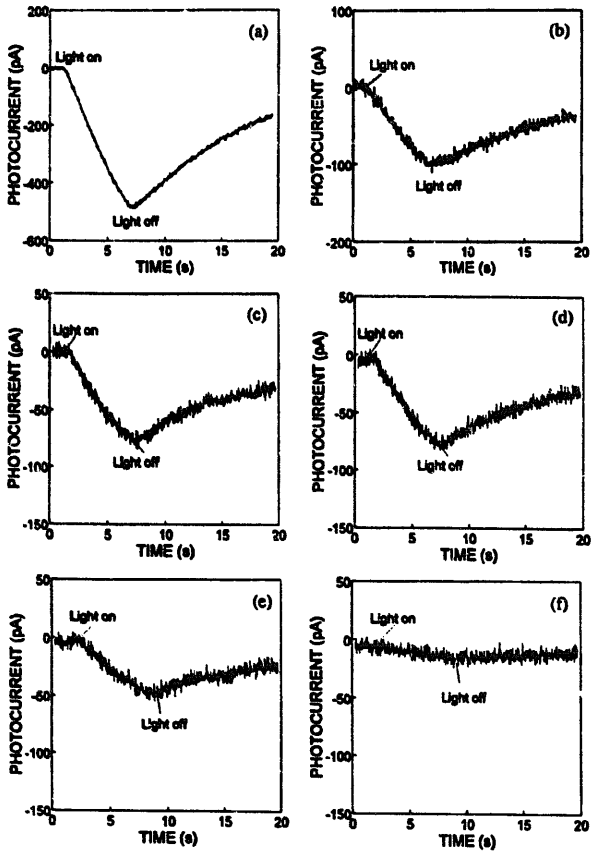

Fig. 5. Kinetics of photocurrent generation and decay in asymmetric LC cell with merocyanine. Light wavelength: (a) 400 nm; (b) 450 nm; (c) 525 nm; (d) 575 nm; (e) 589 nm; (f) 700 nm ($\tau_g \approx 4.1$–4.5 s, $\tau_d \approx 11$–14 s).

The results obtained on changing the side of illumination in both types of cell show that both types of cell are asymmetric, but the degree of asymmetry is much higher for the cell with the metal and semiconducting electrodes than for the cell with two semiconducting electrodes.

The kinetics of signal generation and decay for the sample with merocyanine illuminated at various wavelengths are shown in Fig. 5. The amplitudes are dependent on the amount of absorbed light and therefore the kinetic slopes are not identical for the various wavelengths of illumination. At a higher density of absorbed quanta, e.g. in the region of the protonated form, the increase in the signal amplitude is faster than in the low absorption region of the free base form of the dye. Differences are observed between the kinetics of unpigmented cells (Fig. 3) and merocyanine cells (Fig. 5) and between merocyanine and Chl LC cells (Fig. 4). The photocurrent generation times (τ_g) and decay times (τ_d) are given in Figs. 3–5. From Fig. 5 and Fig. 2(B) (curve 2), it can be concluded that both forms of merocyanine can generate a photocurrent, but with various efficiencies. At 700 nm, where the dye and LC do not absorb, current is not generated (Fig. 5(f)). Comparing the photocurrent amplitude of the same solution with the same illumination, but at various cell thicknesses (Fig. 6), we can see that the amplitude of the 10 μm cell is the highest, much higher than that at 20 μm.

The decrease in the photocurrent amplitude with increasing cell thickness shows that only a thin layer of sample in the vicinity of the semiconducting electrode is active. The amplitude increases slightly at 60 μm thickness. The results presented in Fig. 6 are in agreement with the data reported by Sato [24], who has shown that the current intensity measured decreases with increasing spacer thickness, and the kinetics of current decay are different for various spacers. The small increase in the amplitude observed in our experiment for the 60 μm cell may be due to a change in kinetics with varying spacer thickness. The strong decrease in the current amplitude with an increase in the thickness of the LC layer suggests that

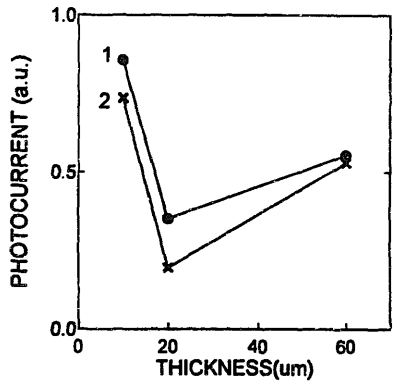

Fig. 6. Photocurrent dependence on cell thickness for Chl *a* in LC: curve 1, $\lambda = 425$ nm; curve 2, $\lambda = 675$ nm.

diffusion of the ions formed at the semiconducting electrode across the cell occurs, rather than only a small replacement of the charge.

A linear dependence of the current signal on the light intensity was observed (not shown). At the light intensity used, practically only monophotonic effects occur.

3.2. *Laser flash experiments*

The kinetics of decay of the signal due to laser flash illumination are very complex, and dependent on the nature of the dye and the light energy absorbed by the sample. The results for the Au/In_2O_3 cell with Chl *a* illuminated by the DCMLC 65001 dye laser (maximum, 658 nm) are presented in Fig. 7. Up to 0.07 ms, the signal increases; it then decreases reaching a minimum at 0.7–1.0 ms; it then increases again with a maximum in the region 12–20 ms; this is followed by another decrease with a flat minimum at about 2000 ms and a slow increase to the starting value. After 50 000 ms, this value has still not been attained. The decay time of the signal is $\tau_d = 16$ s. The time evolution of the signals after illumination of the same sample with the rhodamine 6G dye laser (maximum, 580 nm) (Fig. 8) and the stilbane 3 dye laser (results not shown) exhibits a qualitatively similar behaviour, but the exact positions of the maxima and minima of the signal are not identical. The three illuminations differ in their laser peak energies (DCMLC 65001, 680×10^{-6} J; rhodamine 6G, 1200×10^{-6} J; stilbane 3, 270×10^{-6} J) and in their absorption wavelengths. From the photocurrent action spectra (Fig. 2(A)), it can be seen that the illumination of the sample is less effective for rhodamine 6G than for DCMLC 65001. As a result of the different flash intensities compensated by the various light absorptions, similar numbers of quanta are absorbed in both cases. The Chl *b* photocurrent kinetics (not shown) are similar to the kinetics observed for Chl *a*.

Much simpler kinetics are obtained for mainly protonated merocyanine on illumination with the DCMLC 65001 dye laser (658 nm) (Fig. 9). Only one maximum in the time range 0.07–0.1 ms is formed and in several milliseconds the initial value of the current is restored.

The complex kinetics observed for both Chls are not related to certain specific properties of these pigments, because Sato and Fukuda [22] obtained very similar complex changes in the photocurrent for a nematic crystal with methyl red. In the

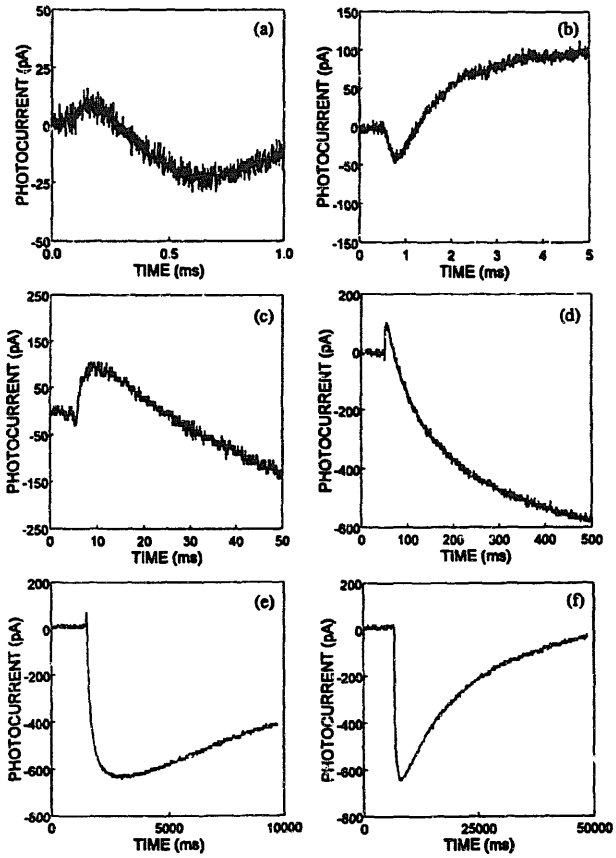

Fig. 7. (a)–(f) Time evolution of the photocurrent signal generated by DCMLC 65001 dye laser (maximum, 658 nm) in asymmetric cell with Chl *a* in LC. Time ranges are given (last $\tau_d \approx 16$ s).

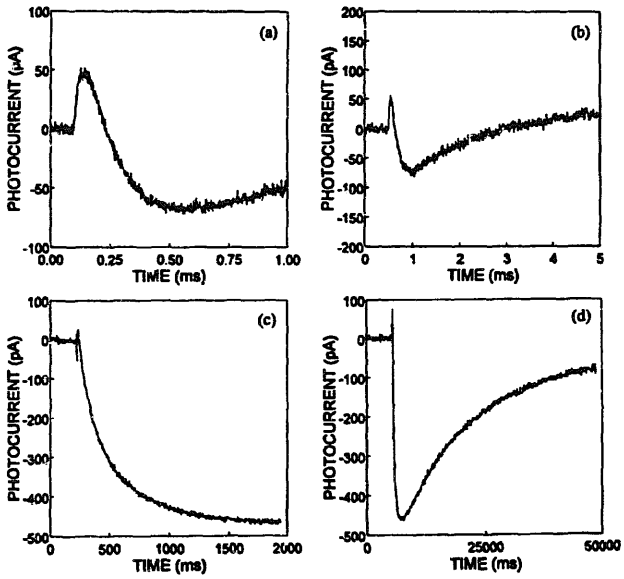

Fig. 8. Photocurrent signal generated by rhodamine 6G laser flash in asymmetric cell with Chl *a* in LC observed in various time ranges (last $\tau_d \approx 20$ s).

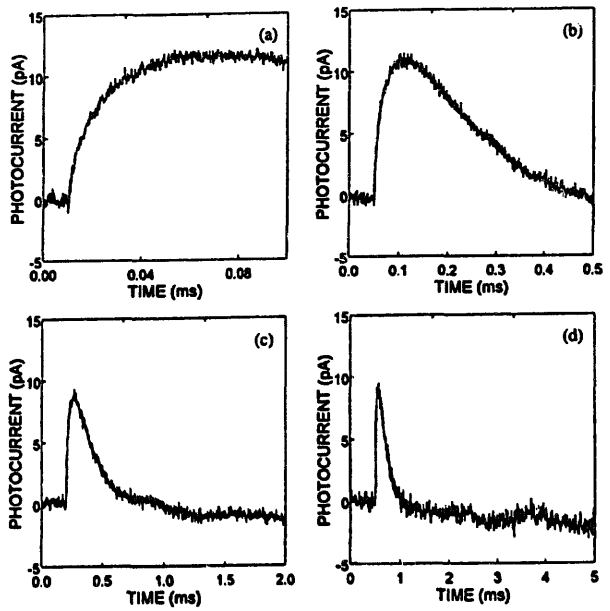

Fig. 9. Photocurrent signal generated by DCMLC 65091 dye laser flash in asymmetric cell with merocyanine in LC observed in various time ranges ($\tau_g \approx 0.01$ ms, $\tau_d \approx 0.2$ ms).

experiment performed by Sato and Fukuda [22], a tungsten lamp with a shutter was used and the signal was recorded by digital wave memory with a sampling time of 1 ms. Only UV radiation was cut out by the filter. In our experiments, the sample was illuminated by a definite wavelength and we were able to measure shorter signals. In both cases (Chls and methyl red) complex processes occur. These effects could be related to the following mechanisms: charge generation in the part of the pigment located near to the electrode; reorientation of the LC and pigment molecules due to the electric field generated by this charge; diffusion of the ions formed through the cell. The slowest peaks, as proposed in Ref. [22], may be due to ion migration. The slow photocurrent effects may also be due to multistep electron transfer between molecules of slightly different redox potential, as observed for polyporphyrin films [31]. The redox potentials of molecules located at various distances from the semiconducting electrode are different because of the various electric fields in the different regions. Chls and merocyanines are different in that merocyanines are highly protonated; therefore, even before illumination, some charged species are present in the whole volume of the cell. Illumination only causes a change in the charge of the molecules located near to the electrode. Both protonated and free base molecules take part in the tunnelling of electrons to the electrode, but the free base form is more efficient. It seems that, in the case of Chl *a* and methyl red [24], the charges are predominantly formed as a result of illumination at the semiconducting electrode, and this process is followed by several secondary processes, e.g. charge migration, etc. For the merocyanine sample, these secondary slow processes are decreased because of the charge present in the dark over the whole volume of the sample. In such samples, the effect is predominantly due to charge displacement in the vicinity of the semiconducting electrode in the electric field gradient.

Light-induced charge motions similar to those observed for Chl in LC occur in several biological systems, such as photosynthetic organisms containing Chls [3,4,6] and in purple membranes of *Halobacterium* [26–28,32]. Charge separation and displacement can be observed using several spectroscopic methods, and directly by measurement of the photopotential or photocurrent [3,4,6]. The differences between the photoelectrical results obtained for aqueous and dry samples [3,4,6,26–28] may suggest that the photovoltage is affected by the structure of the membrane system [3]. This is also suggested by the different electrical signals observed in "face-aligned" and "edge-aligned" chloroplasts [7].

4. Conclusions

1. The model investigated exhibits certain common properties with biological systems containing chains of electron donors and acceptors. In our model, the semiconducting electrode with its associated electric field gradient plays the role of electron acceptor. The system used provides an opportunity to follow the photocurrent kinetics in the microsecond time range. Over this time scale, electrochemical cells containing Chls in LC exhibit complex photocurrent kinetics generated by laser flash photolysis, which are similar to some extent to those observed for chloroplasts [2]. These kinetics are due to the fluid, oriented LC matrix which, in our experiments, mimics the biological membrane. In this matrix, the ions photogenerated in the vicinity of the junction between the semiconducting electrode and the sample migrate.
2. In the case of Chls, charge displacement and the flow of charge to the semiconducting electrode are observed as well as slow processes probably due to the different velocities of migration of different charges in the LC cell and/or multistep electron transfer between molecules.
3. The charge distribution in the whole volume in a dark sample, as observed for protonated merocyanine, prevents ion migration between the electrodes. As a result, only one photocurrent peak due to charge displacement in the region of the semiconducting electrode is observed.
4. In our experimental conditions, the role of the light gradient can be neglected in comparison with the effect of the asymmetric properties of the cell electrodes. This shows that, without a light gradient, which plays a crucial role in biological systems [3,4,6], a strong photocurrent can be generated by visible light in Chl molecules located in an anisotropic matrix with an additional gradient of the electric field. Such conditions can also be fulfilled for Chls in organisms; therefore the influence of part of the pigment molecules on photoionization must be taken into account in an analysis of the photopotential of photocurrent kinetics.

5. It has also been shown that the distribution of charged molecules in the matrix in which the pigment is located may have an influence on the kinetics of photoelectrical effects. It seems that the membrane fluidity and structure, as well as the distribution of charged species, may have an effect on the photoelectrical properties of biological samples.

Acknowledgements

A.P. thanks the European Science Foundation (Programme "Biophysics of Photosynthesis") for a short-term travel grant and Poznan University of Technology for Grant DS 62-120/2. D.F. wishes to thank the Polish Committee for Scientific Research for KBN Grant No. PB 339/PO4/95/08. N.S.N. is grateful for a Doctoral Fellowship from the Polish Ministry of Science and Education.

References

[1] C.F. Fowler, B. Kok, Biochim. Biophys. Acta 357 (1974) 308.
[2] H.W. Trissl, U. Kunze, W. Jung, Biochim. Biophys. Acta 682 (1982) 364.
[3] H.W. Trissl, J. Breton, J. Deprez, W. Leibl, Biochim. Biophys. Acta 893 (1987) 305.
[4] A. Dobek, J. Deprez, G. Paillotin, W. Leibl, H.W. Trissl, J. Breton, Biochim. Biophys. Acta 1015 (1990) 313.
[5] G. Paillotin, A. Dobek, J. Breton, W. Leibl, H.W. Trissl, Biophys. J. 66 (1993) 379.
[6] K. Barabas, G. Varo, L. Keszthelyi, J. Photochem. Photobiol. B: Biol. 26 (1994) 37.
[7] Sz. Osvath, M. Meszena, V. Barzda, G. Garab, J. Photochem. Photobiol. B: Biol. 26 (1994) 207.
[8] D. Frąckowiak, S. Hotchandani, R.M. Leblanc, Photobiochem. Photobiophys. 6 (1983) 339.
[9] D. Frąckowiak, D. Bauman, H. Manikowski, W.R. Browett, M.J. Stillman, Biophys. Chem. 28 (1987) 101.
[10] A. Ptak, E. Chrzumnicka, A. Dudkowiak, D. Frąckowiak, J. Photochem. Photobiol. A: Chem. 98 (1996) 159.
[11] A. Ptak, E. Chrzumnicka, A. Planner, D. Frąckowiak, Biophys. Chem., in press.
[12] D. Frąckowiak, S. Hotchandani, R.M. Leblanc, Photobiochem. Photobiophys. 7 (1984) 41.
[13] D. Wróbel, Biophys. Chem. 26 (1987) 91.
[14] D. Frąckowiak, D. Bauman, M.J. Stillman, Biochim. Biophys. Acta 681 (1982) 273.
[15] I. Gruda, S. Hotchandani, D. Frąckowiak, Photobiochem. Photobiophys. 12 (1986) 267.
[16] J. Goc, D. Frąckowiak, J. Photochem. Photobiol. A: Chem. 51 (1991) 233.
[17] D. Frąckowiak, M. Niedbalska, M. Romanowski, I. Gruda, Stud. Biophys. 123 (1988) 135.
[18] D. Frąckowiak, M. Romanowski, S. Hotchandani, L. Leblanc, R.M. Leblanc, I. Gruda, Bioelectrochem. Bioenerg. 19 (1988) 371.
[19] H.T. Witt, Biochim. Biophys. Acta 505 (1979) 355.
[20] H.T. Witt, in Grovindjee (ed.), Bioenergetics of Photosynthesis, Academic Press, New York, San Franciso, London, 1975, Chapter 10, pp. 495–551.
[21] J. Goc, M. Hara, T. Tateishi, J. Miyake, J. Photochem. Photobiol. A: Chem. 93 (1996) 137.
[22] S. Sato, S. Fukuda, Mol. Cryst. Liq. Cryst. 98 (1983) 99.
[23] H. Kamei, Y. Katayama, T. Ozawa, Jpn. J. Appl. Phys. 11 (1972) 1385.
[24] S. Sato, Jpn. J. Appl. Phys. 20 (1981) 1989.
[25] K. Iryama, N. Ogura, A. Takamiya, J. Biochem. 76 (1974) 901.
[26] G. Varo, L. Keszthleyi, Biophys. J. 43 (1983) 47.
[27] S.G. Hristova, G. Varo, A. Der, Acta Biochim. Biophys. Acad. Sci. Hung. 19 (1984) 215.
[28] R. Toth-Boconadi, S.G. Taneva, L. Keszthelyi, Biophys. J. 67 (1994) 2490.
[29] D. Frąckowiak, B. Zelent, H. Malak, R. Cegielski, J. Goc, M. Niedbalska, A. Ptak, Biophys. Chem. 54 (1995) 95.
[30] N.S. Naser, A. Planner, D. Frąckowiak, J. Photochem. Photobiol. A: Chemistry, submitted for publication.
[31] G.W. Rayfield, D.T. Friesen, D. Lorentz, C. Wamser, in: F.T. Hong (Ed.), Molecular Electronics, Biosensors and Biocomputers, Plenum, New York, London, 1989, p. 149.
[32] D. Frąckowiak, C. Jadźyn, Bull. Acad. Polon. Sci. Ser. Biol. 27 (1980) 523.